

Supporting Information for

Influence of albumin configuration by the chiral polymers-grafted gold nanoparticles

Jun Deng, Zheng Li, Mengyun Yao, Changyou Gao*

MOE Key Laboratory of Macromolecular Synthesis and Functionalization, Department of Polymer

Science and Engineering, Zhejiang University, Hangzhou 310027, China.

*Corresponding author.

Email: cygao@mail.hz.zj.cn

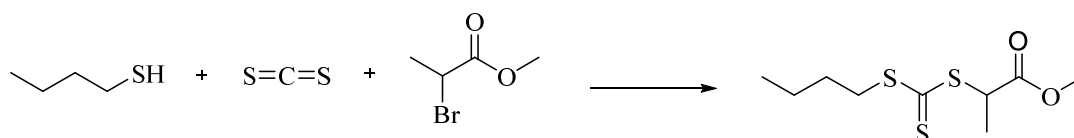
Fax: +86-571-87951108

Materials and methods

Materials

L-Valine, D-valine, 1-butanethiol, carbon disulfide (CS₂), ethyl 2-bromopropionate, methyl-2-bromopropionate and acryloyl chloride were purchased from Aladdin company. Triethylamine (TEA), dimethyl formamide (DMF) and dichloromethane (DCM) were obtained from Sinopharm Chemical Reagent Co., Ltd, which were vacuum-distilled prior to use. Other chemical reagents were purchased from Sinopharm Chemical Reagent Co., Ltd and used without purification.

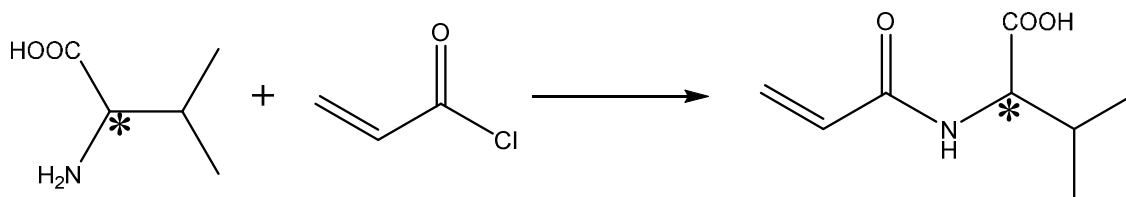
Synthesis and characterization of methyl 2-(butylthiocarbonothioylthio)propanoate (MCEBTTC)



Scheme S1. Synthesis of RAFT agent of MCEBTTC.

The MCEBTTC was synthesized according to the procedures reported previously ([Scheme S1](#))¹ and characterized by H-NMR. ¹H NMR (CDCl₃) CH₃ δ 0.92 (*t*, 3H), CH₂ δ 1.43 (*m*, 2H), CH₃ δ 1.62 (*d*, 3H), CH₂ δ 1.65 (*q*, 2H), CH₂ δ 3.36 (*t*, 2H), CH₃ δ 3.73 (*s*, 3H), CH δ 4.84 (*q*, 1H).

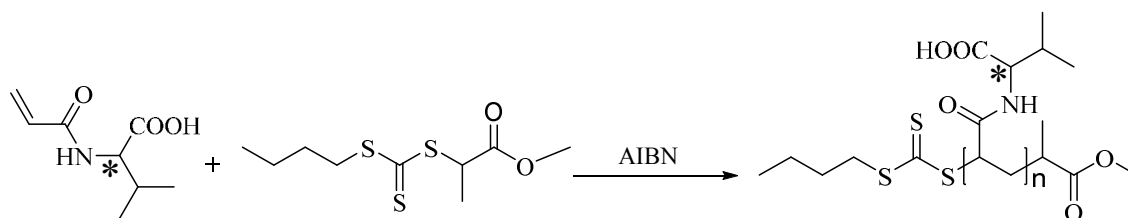
Synthesis and characterization of acryloyl-L(D)-valine monomers



Scheme S2. Synthesis of acryloyl-L(D) -valine monomers.* represents chiral center.

The acryloyl-L(D)-valine monomers were synthesized according to the procedures reported previously (Scheme S2) ². Their structure was verified by ¹H NMR (CDCl₃). CH₃ δ 0.89 (*d*, 6H), CH δ 2.11 (*m*, 1H), CH δ 4.31 (*d*, 1H), CH δ 5.58 (*t*, 1H), CH₂ δ 6.17, 6.28 (*m*, 2H).

Synthesis and characterization of poly(acryloyl-L(D)-valine)



Scheme S3. Schematic illustration of synthesis of poly(acryloyl-L(D)-valine) (L(D)-PAV).* represents chiral center.

The poly(acryloyl-L(D)-valine) (L(D)-PAV) molecules were synthesized *via* the reversible addition-fragmentation chain transfer polymerization (RAFT) method (Scheme S3). Briefly, methyl 2-(butylthiocarbonothioylthio)propanoate (50.4 mg), azodiisobutyronitrile (AIBN, 3.4 mg) and acryloyl valine (1.37 g) were dissolved in 5 mL *N,N*-dimethylformamide (DMF). The mixture was deoxygenated by purging with nitrogen for 20 min, and then heated at 70 °C for 4 h. The reaction was stopped by exposure to air. The mixture was precipitated in excess diethyl ether, and then separated by centrifugation. The dissolution and precipitation cycle was repeated 3 times. The polymers were dried under high vacuum for 48 h at room temperature to give a yellow solid product. The product was characterized by Gel Permeation Chromatography (GPC, THF, Waters 1515 Isocratic HPLC). The

weight average molecular weight (M_w) of L-PAV and D-PAV was 3580 g/mol and 3611 g/mol, and narrow polydispersity (D) of 1.14 and 1.15, respectively (Figure S1a,b).

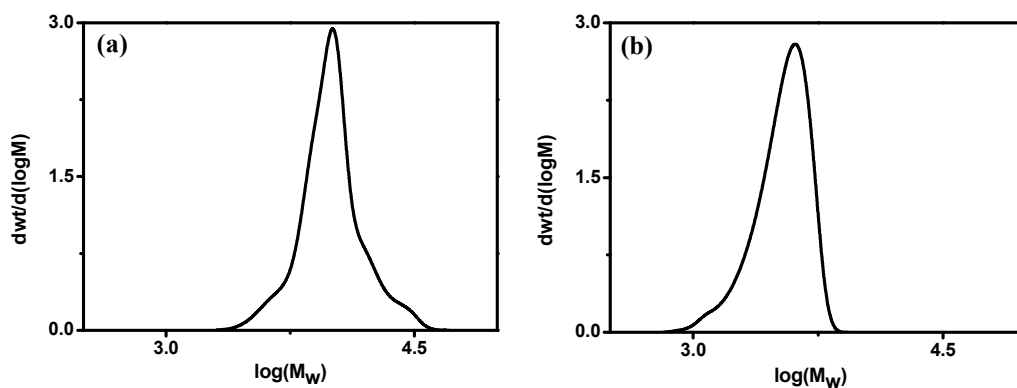


Figure S1. GPC curves of (a) L-PAV and (b) D-PAV.

Size distribution

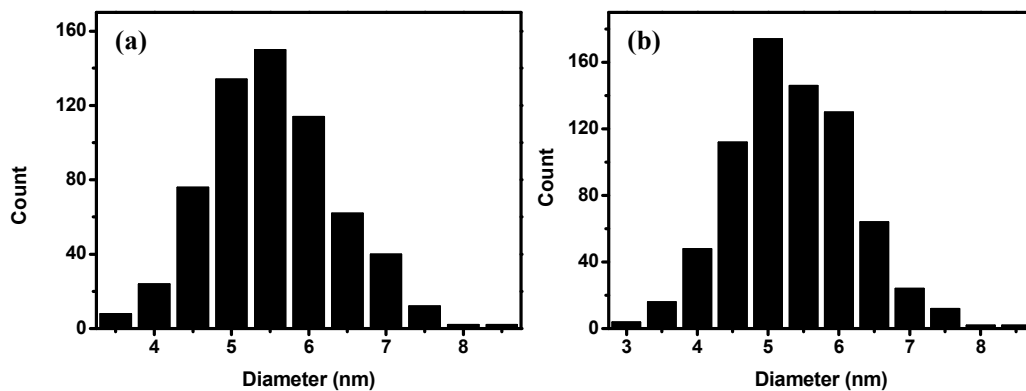


Figure S2. Size distribution calculated for (a) L-PAV-AuNPs and (b) D-PAV-AuNPs from TEM images (Based on random counting of more than 600 particles).

Conjugate characterization

The different concentrations of PAV-AuNPs (0-0.05 μM) were incubated in 0.15 μM BSA/PBS solution under shaking for 72 h. The images of these solutions were obtained using a digital camera.

Clear red color of these samples means excellent dispersion of gold nanoparticles (Figure S3a,b).

The effect of proteins on the plasmon excitation wavelength of the PAV-AuNPs was determined in the absence and presence of BSA on a UV-Vis spectrophotometer (Shimadzu UV2550), respectively. Each spectrum was an average of 3 individual samples recorded twice at 25 $^{\circ}\text{C}$ (Figure S3c,d).

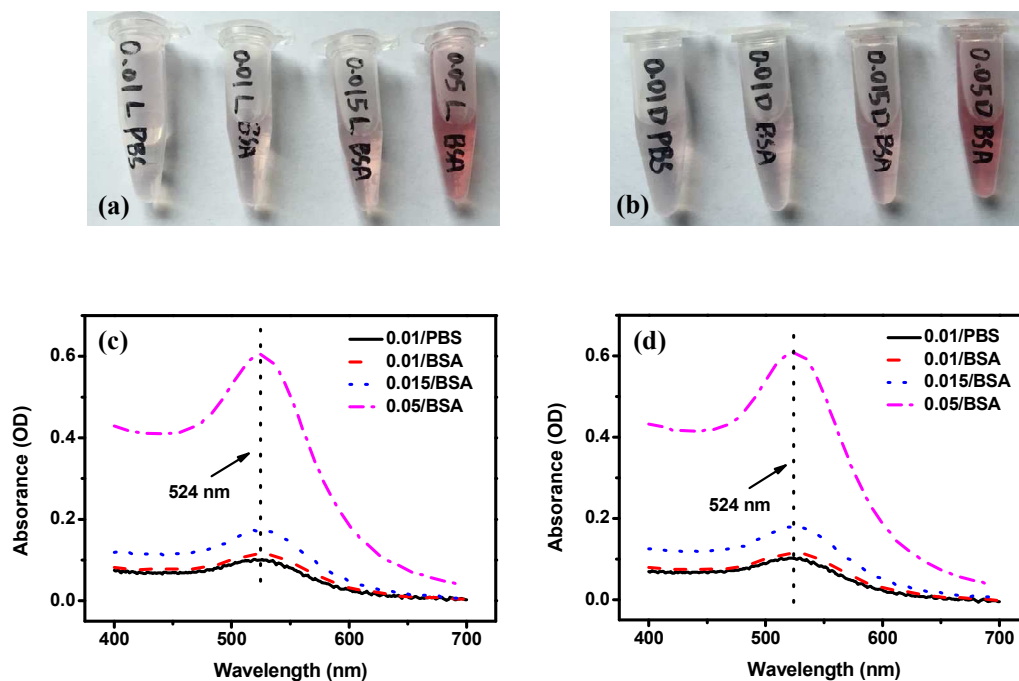


Figure S3. (a,b) Digital images and (c,d) UV-vis spectra of 0.01 and 0.05 μM of (a,c) L-PAV-AuNPs and (b,d) D-PAV-AuNPs in PBS and 0.15 μM BSA/PBS solution, respectively.

TEM images

The dispersion state of BSA-conjugated L-PAV-AuNPs and D-PAV-AuNPs was determined by TEM

(H-7650, [Figure S4](#)). 0.01 μM L-PAV-AuNPs or D-PAV-AuNPs was incubated in 0.15 μM BSA/PBS under shaking for overnight at 25 $^{\circ}\text{C}$. Then 15 μL of diluted solution was applied on a carbon-coated copper grid, and dried under atmosphere overnight. Nearly 20 μL water was dropped on the carbon-coated copper grid, and blotted quickly. This process was repeated twice. Finally the carbon-coated copper grid was dried under atmosphere overnight.

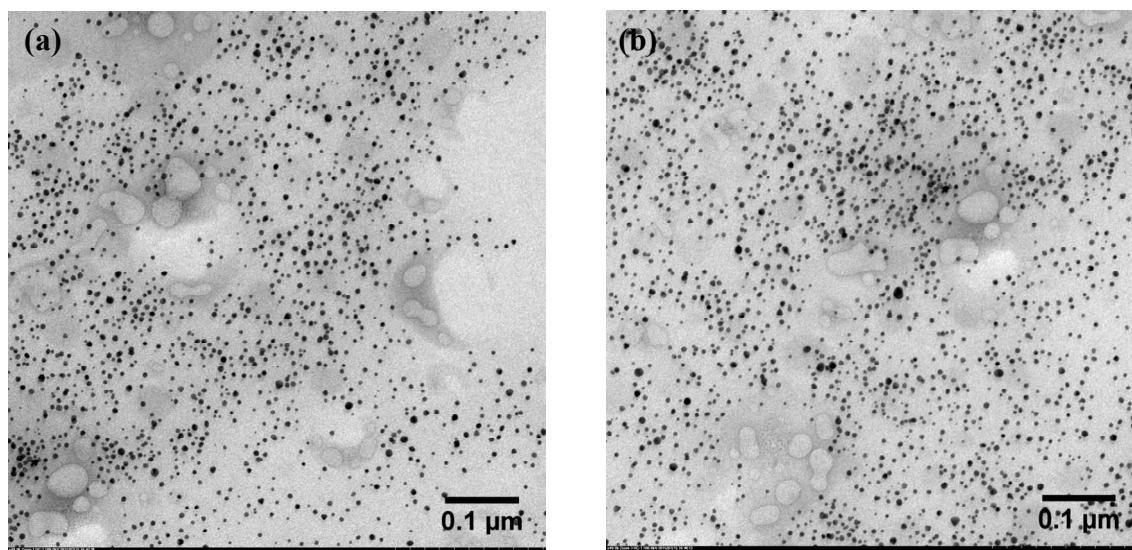


Figure S4. TEM images of 0.01 μM of (a) L-PAV-AuNPs and (b) D-PAV-AuNPs being incubated in 0.15 μM BSA/PBS solution.

Fluorescence analysis

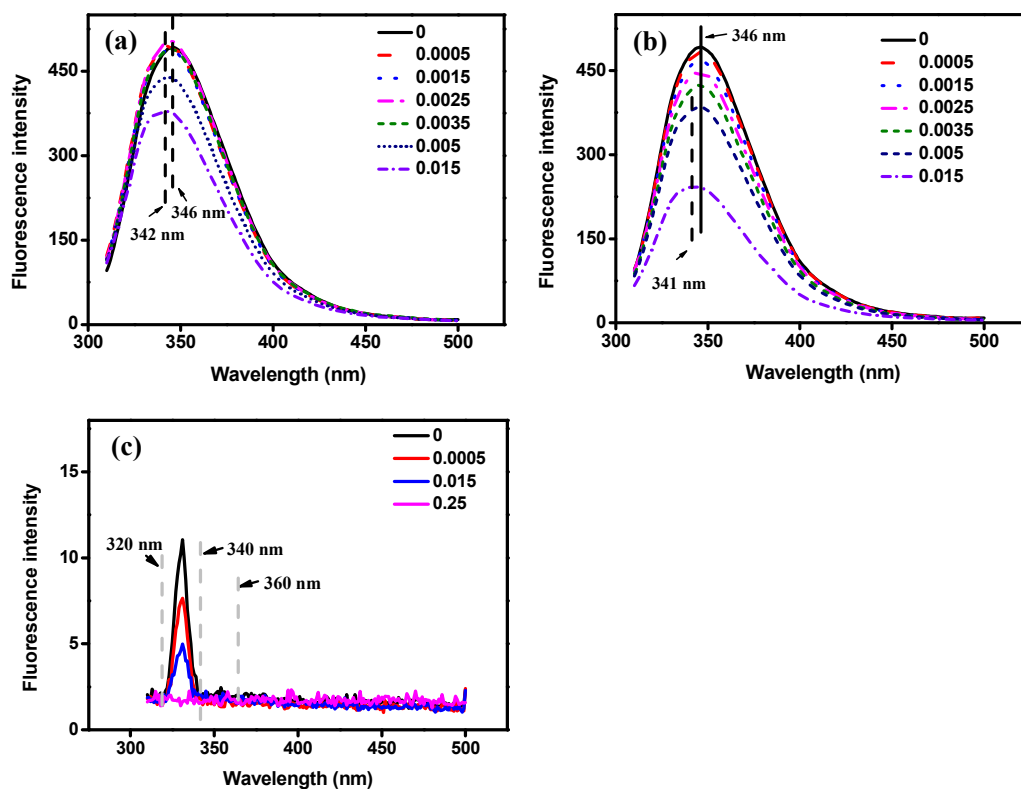


Figure S5. Tryptophan fluorescence emission of BSA (0.15 μM) containing 0~0.015 μM of (a) L-PAV-AuNPs and (b) D-PAV-AuNPs, respectively. (c) The fluorescence emission spectra of water and AuNPs of different concentrations without PAV grafting.

After being incubated with PAV-AuNPs, the fluorescence intensity of BSA decreased gradually with the increase of PAV-AuNPs concentration (Figure S5 a,b). Moreover, the peak of the tryptophan fluorescence emission of BSA in the presence of PAV-AuNPs was blue-shifted (Figure S5 a,b). Even being incubated in the 0.015 μM PAV-AuNPs (The largest concentration of NPs used here), the peak of the tryptophan fluorescence emission of BSA was still above 340 nm (Figure S5 a,b). As shown in Figure 5c, the water had a peak of fluorescence emission at 330 nm due to the Raman scattering³. The peak intensity at 330 nm was significantly decreased with the addition of AuNPs (Figure S5c), which

possibly means that the AuNPs could decrease the Raman scattering. When the concentration of AuNPs increased to $0.25\ \mu\text{M}$, no emission peak existed. These results suggest that the AuNPs had no fluorescence emission between 310-500 nm upon being excited at 295 nm. Moreover, the emission intensity of the AuNPs at 320 nm and above 340nm ($<500\ \text{nm}$) did not change with the increase of AuNPs concentration (Figure S5c).

ITC analysis

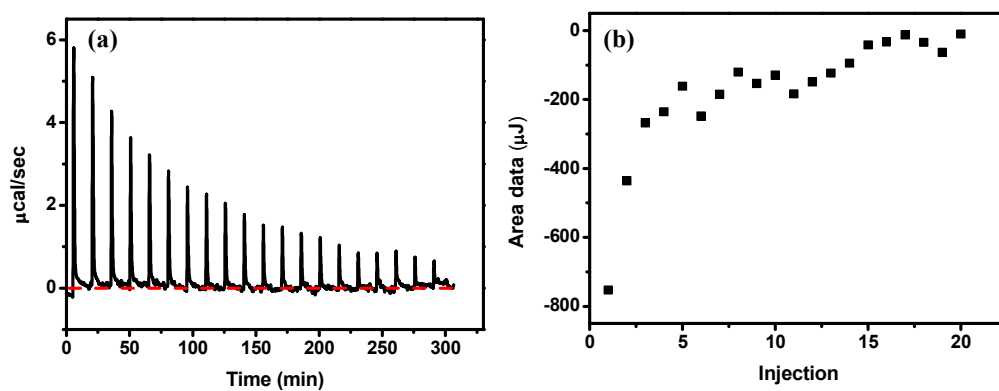


Figure S6. (a) Heat flow (ITC data) during the titration of $500\ \mu\text{M}$ BSA into $10\ \text{mM}$ $7.4\ \text{PBS}$ at $25\ ^\circ\text{C}$.

(b) The evolved heat per injection of BSA.

References:

- (1) Truong, N. P. Self-catalyzed degradation of linear cationic poly(2-dimethylaminoethyl acrylate) in water. *Biomacromolecules* **2011**, 12, 1876-1882.
- (2) Ezell, R. G.; Gorman, I.; Lokitz, B.; Ayres, N.; McCormick, C. L. Stimuli-responsive ampholytic terpolymers of N-acryloyl-valine, acrylamide, and (3-acrylamidopropyl)trimethylammonium chloride: synthesis, characterization, and solution properties. *J. Polym. Sci. Polym. Chem.* **2006**, 44, 3125–3139.
- (3) Gao, Y.; Wang, X.; Tong, L.; Qin, A.; Sun, J. Z.; Tang, B. Z. A new strategy of post-polymerization modification to prepare functionalized poly(disubstituted acetylenes). *Polym. Chem.* **2014**, 5, 2309-2319.